Letters

A Family of Bridgeless Quasi-Resonant LED Drivers

D. Shmilovitz, *Member, IEEE*, A. Abramovitz, *Member, IEEE*, and I. Reichman

***Abstract*—A family of offline bridgeless quasi-resonant LED drivers is introduced. The prominent features of the proposed drivers are the capacitive isolation feature, inherent low line-current distortion, and high power factor. The concept is validated by a 30-W prototype operated in the range of 150–200 kHz and 30-V dc output (LED string voltage).**

***Index Terms*—Bridgeless circuits, LED lamps, switching circuits, soft switching.**

I. Introduction

DEPLOYMENT of offline LED lighting systems can bring many benefits—LEDs have better durability, longer life, and much higher energy efficiency than the incandescent lighting. LED lighting can help energy conservation and reduce CO_x emissions worldwide [1]. LEDs require specialized LED drivers. The LED driver is a low-power offline ac–dc converter, which supplies the LED string with a required operating voltage and current. Implementation of compact, high performance, and low-cost LED drivers is quite challenging, since the LED driver converter may have many power processing and control features onboard, has to comply with numerous safety regulations, and is a major contributor to the cost of a LED lighting fixture. For these reasons, the development of affordable LED drivers is gaining priority.

LEDs are low temperature devices and require heat management. Metal heatsinks and casing may become a safety hazard. Therefore, safety standards [2] should be considered. Several authors have investigated capacitive isolation feature as an alternative to the usual but bulky isolation transformer [3]–[7]. A discussion of the touch current of a capacitively isolated equipment is presented in [3]. As an example, it was evaluated in [4] that the leakage current flowing through a 10-nF capacitor from 60-Hz mains is less than 1 mA. This suggests that capacitive safety barrier can be made effective.

This letter further extends the ideas of capacitively isolated LED drivers [5] [6], and introduces and briefly describes the principles of related bridgeless variants of this approach.

Manuscript received July 15, 2015; revised August 6, 2015; accepted August 15, 2015. Date of publication August 28, 2015; date of current version November 16, 2015. This work was supported in part by GE Lighting Israel, Ltd., under Grant 30040000000.

The authors are with the School of Electrical Engineering, Tel-Aviv University, Tel-Aviv 69978, Israel (e-mail: shmilo@post.tau.ac.il; alabr@hotmail.com; isarreic@post.tau.ac.il).

Color versions of one or more of the figures in this paper are available online at http://ieeexplore.ieee.org.

Digital Object Identifier 10.1109/TPEL.2015.2470600

II. Basic Principles

A. Basic Topology

LEDs should be driven by current sources, suggesting that the converter should exhibit gyrator characteristics [8], [9]. The basic configuration of the proposed bridgeless quasi resonant LED driver (BL-QRLEDD) is illustrated in Fig. 1(a). BL-QRLEDD is a modification of [2] and [3]. The circuit consists of a full-wave totem-pole-type bridgeless rectifier D_1, D_2,M_1, M_2 switching an input inductor L_i and a pair of *small* series capacitors $2C_s$. Diodes D_5, D_6 are used to steer the capacitor current either into the small resonant inductor L_r or into the filter capacitance $C_{\rm LED}$, across which a series string of LEDs is connected. The task of D_5 is to prevent the parasitic oscillation between the switch capacitance and L_r.

B. Implementation of Constant $T_{\rm on}$ control

One possible switching strategy to control the BL-QRLEDD is driving both M_1 and M_2 by the same switching signal with constant on-time and variable frequency. Another possible modulation approach is turning the M_2 switch-on for the entire duration of the positive-line half cycle, while delivering a constant $T_{\rm on}$ gating pulse to M_1. During the negative-line half cycle the roles of M_1 and M_2 are interchanged. The advantages of the first approach are that it requires no line synchronization and the switches can share the off-state voltage, whereas the merit of the second approach is the lower resistance of the L_i discharge path.

C. Principle of Operation

The topology of the BL-QRLEDD is somewhat similar to SEPIC, yet, BL-QRLEDD is a quasi-resonant converter and operates differently. BL-QRLEDD family in Fig. 1 exploits the advantage of the discontinuous conduction mode (DCM) of the input current, which has the merit of the average input current closely following the line voltage. Detailed analysis will be given elsewhere; in brief, however, during the switch turned ON, the input inductor L_i is linearly charged from the rectified line voltage, while L_r resonates and captures most of the energy stored in C_s capacitance. Upon switch turned OFF, which occurs under zero-voltage condition, L_i recharges the $2C_s$ capacitors, while L_r transfers all of the captured energy to the output capacitor $C_{\rm LED}$.

Totem-pole bridgeless rectifiers are less popular due to the associated reverse-recovery problems. Creating DCM operation conditions for L_r inductor guaranties zero-current turn-off of the output rectifier and alleviate these problems.

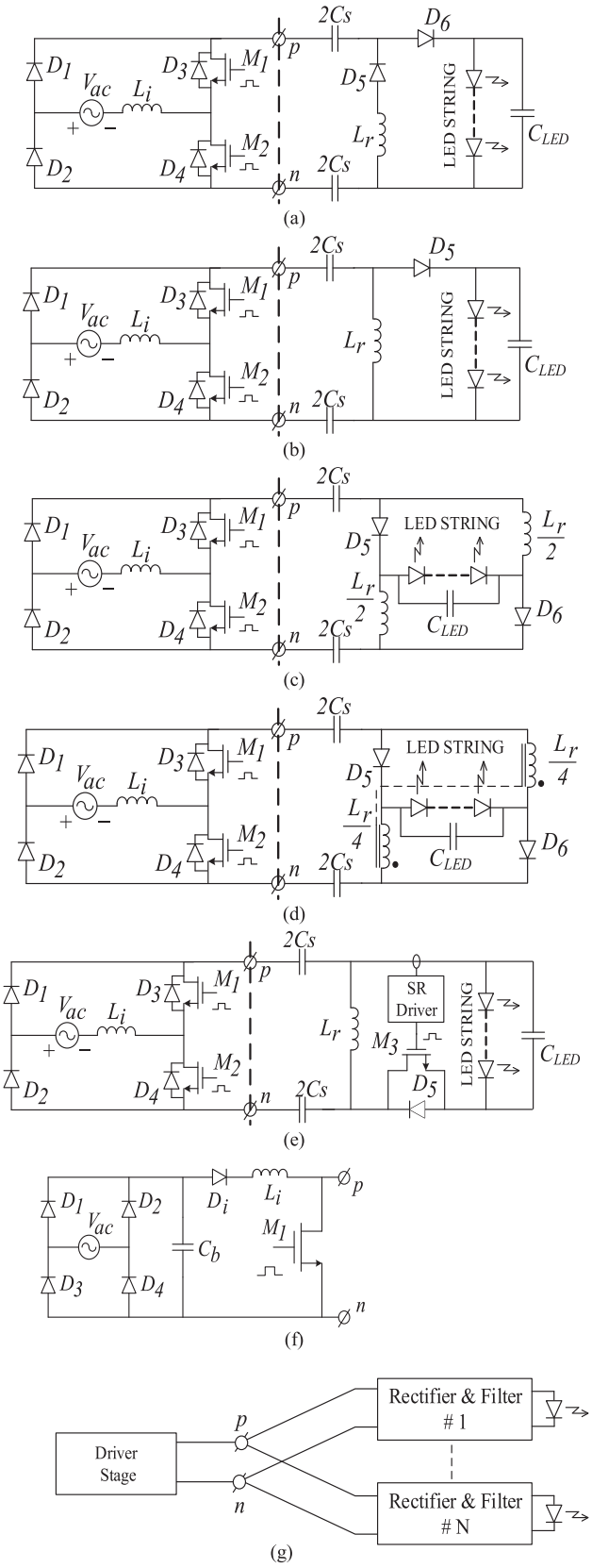

Fig. 1. Proposed BL-QRLEDD family: (a) basic BL-QRLEDD; (b) modified BL-QRLEDD; (c) BL-QRLEDD with current doubler rectifier; (d) BL-QRLEDD with coupled current doubler rectifier; (e) BL-QRLEDD with synchronous rectifier; (f) single-switch front-end for QRLEDD; (g) general concept of the multistring QRLEDD.

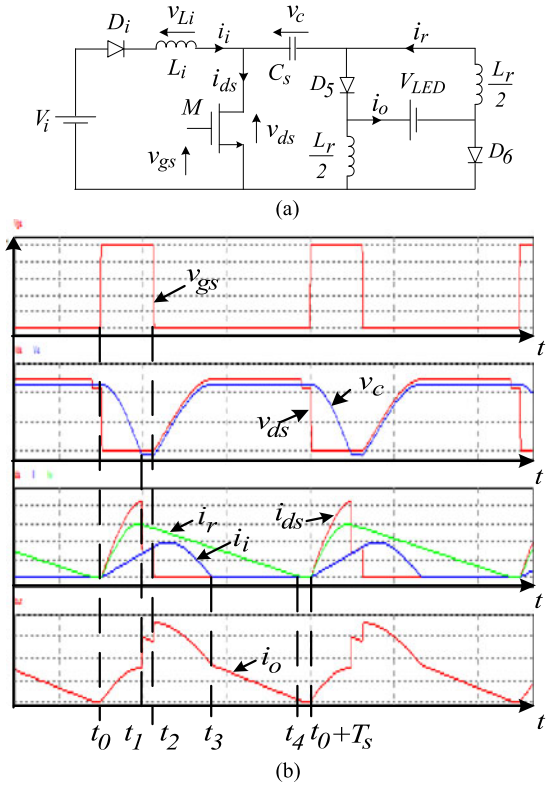

Fig. 2. (a) Equivalent circuit and (b) simulated waveforms of the proposed QRLEDD with coupled current doubler rectifier on the switching cycle scale.

D. Simulation

Equivalent circuit and simulated waveforms of the basic BL-QRLEDD variant are shown in Fig. 2. Here, several topological states can be identified throughout the switching cycle. Examination of the switching waveforms in Fig. 2(b) reveals favourable zero-voltage (ZVS) turn-off and zero-current (ZCS) turn-on switching of the switch, which are a prerequisite to attain high efficiency at high frequency. Evidently, on the line frequency scale, the average line current follows the line voltage; hence, BL-QRLEDD attains resistive input characteristic and has inherent high power factor and low line-current distortion.

III. Derivation of BL-QRLEDD Family

In practice, the voltage drop across D_5 and D_6 in comparison to the LED string voltage cannot be disregarded. In order to alleviate the conduction losses, D_5 can be re moved as shown in Fig. 1(b). The penalty for the increased efficiency is an increased parasitic oscillation, which appears due to the resonance between the switch parasitic capacitance and L_r. The amplitude of the oscillation equals the output voltage $V_{\rm LED}$.

The BL-QRLEDD in Fig. 1(a) encounters conflicting requirements. In order to keep the switch conduction losses and the core losses of L_r at an acceptable level, the resonant charging current of L_r (during the C_s–L_r resonance interval) has to be limited. This implies that the inductor L_r has to be of sufficiently large value. However, higher inductance value extends the discharge time of L_r towards $C_{\rm LED}$. This is undesirable, since it limits

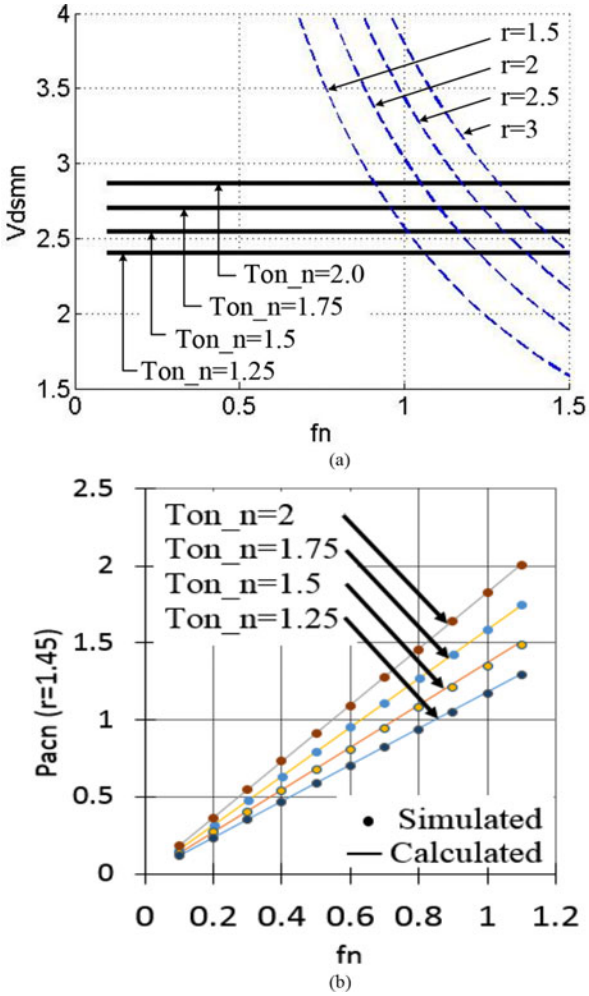

Fig. 3. Calculated indexes of the proposed QRLEDD as a function of the on-time $T_{\rm on}$ and the normalized switching frequency f_n: (a) Normalized peak switch voltage $V_{\rm dsmn}$. (b) Normalized power P_n.

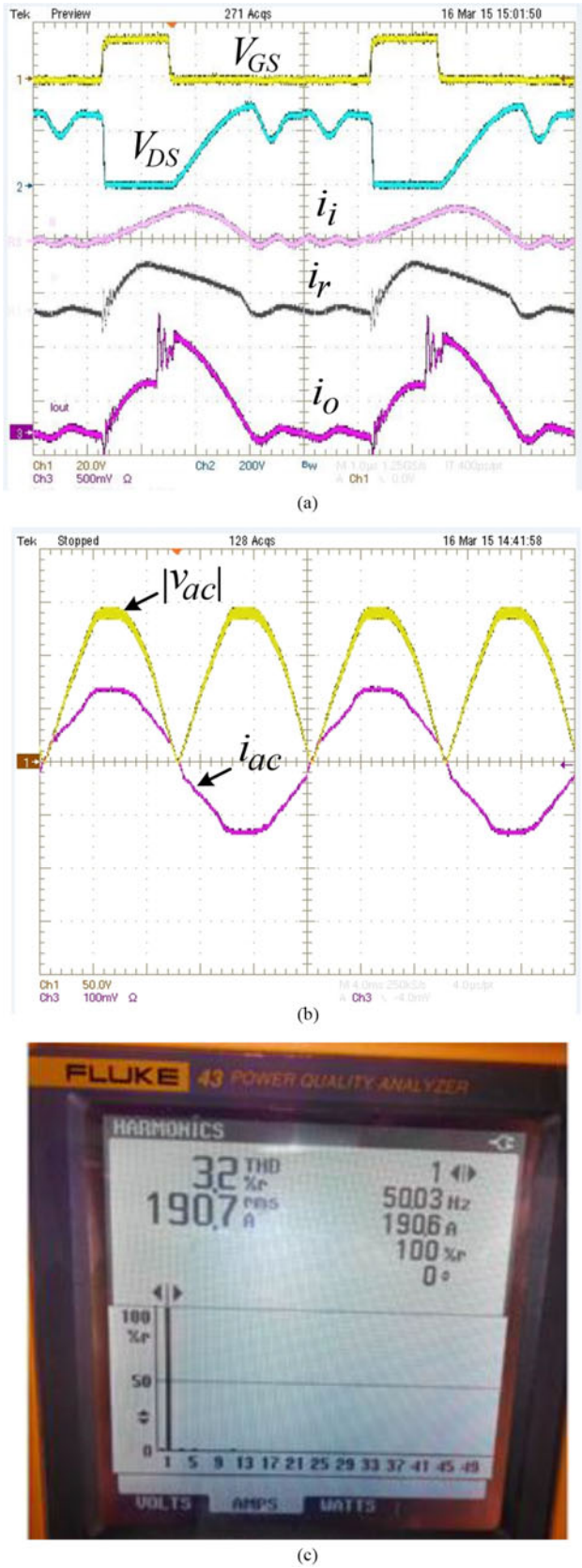

Fig. 4. Typical experimental waveforms of the proposed QRLEDD with coupled current doubler rectifier: (a) On the switching-cycle scale top to bottom: v_{gs} 20 V/div, v_{ds} 200 V/div; i_i, i_r, and i_o 1.5 A/div; horizontal 1.25 μs/div. (b) On the line cycle scale: top- rectified line $|v_{\rm ac}|$ 50 V/div, bottom- $i_{\rm ac}$ 100 mA/div; horizontal 4 ms/div. (c) Measured harmonic spectra and THD [%] of the line current [milliamperes].

the switching frequency and, consequently, converter's output power. The modified circuit in Fig. 1(c) is designed to alleviate this limitation. This configuration is referred to as BL-QRLEDD with current doubler rectifier. Here, C_s resonates with the larger series equivalent L_r and attains lower peak current, while shorter discharge time is attained when both $L_r/2$ are discharged into $C_{\rm LED}$ in parallel. An additional advantage of this circuit is that each diode carries only the half of the output current flowing into $C_{\rm LED}$. A variant of the idea, the BL-QRLEDD with coupled current doubler rectifier, as shown in Fig. 1(d), uses a coupled inductor with 1:1 turn ratio and attains 4:1 series to parallel inductance ratio. To improve the efficiency, albeit at increased complexity and cost, BL-QRLEDD circuits can be modified with synchronous rectifiers (SR), as illustrated in Fig. 1(e). (Any SR driver designed for DCM flyback can be used.) Additional members of the QRLEDD family can be derived by cutting out the bridgeless rectifier in Fig. 1(a)–(e) along the p-n axis, and replacing it with the single-switch arrangement shown in Fig. 1(f). Note the additional fast diode $D_{\rm i}$ in series with the slow line rectifier.

Extending the idea of [7], a general scheme in Fig. 1(g) is suggested to feed multistring LED lamps. The input stage

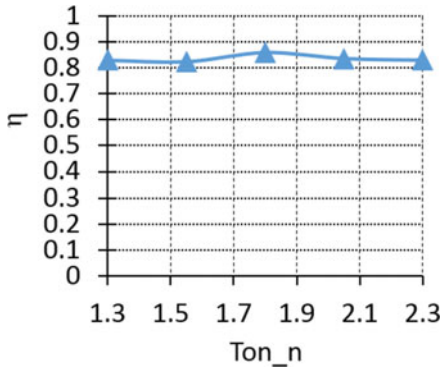

Fig. 5. Efficiency of the experimental prototype.

can either be the single switch or the bridgeless QRLEDD, whereas the output section can be any of the circuits shown in Fig. 1(a)–(e).

IV. Performance Indexes

Preliminary analysis of topology in Fig. 1(d) yields the normalized peak switch voltage

$$V_{\mathrm{dsmn}} = \frac{V_{\mathrm{dsm}}}{\sqrt{2}V_{\mathrm{rms}}} = 1 + \sqrt{1 + \frac{\pi^2}{4r^2}T_{\mathrm{on\_}n}^2} \qquad (1)$$

whereas, the normalized averaged output power P_{av} per line cycle is

$$P_n = \frac{P_{av}}{V_{\mathrm{rms}}^2/2Z_{0i}} = 0.9\left(\frac{f_n}{2\pi}\right)V_{\mathrm{dsmn}}^2\left[1 + 2\frac{V_{Ln}}{V_{\mathrm{dsmn}}}\right] \qquad (2)$$

here V_{rms} is the rms line voltage; $r^2 = L_i/L_r$ is the inductance ratio; T_{on} is the switch-on time; $T_{\mathrm{on\_}n} = 2T_{\mathrm{on}}/\pi\sqrt{L_rC_s}$ is the normalized switch-on time; $V_{Ln} = V_{\mathrm{LED}}/\sqrt{2}V_{\mathrm{rms}}$ is the normalized LED string voltage; $Z_{0i} = \sqrt{L_i/C_s}$ is the characteristic impedance; f_s is the switching frequency; $f_n = f_s/f_{0i}$ is the normalized switching frequency relative to the series resonant frequency $f_{0i} = 1/2\pi\sqrt{L_iC_s}$.

The plots of the normalized peak switch voltage (1) and power (2), as a function of the normalized frequency f_n and normalized switch-on time $T_{\mathrm{on\_}n}$ are shown in Fig. 3. The desired DCM region of the output current lies to the left of the dashed curves in Fig. 3(a). Theoretical prediction stands in good agreement with the simulated results, see Fig. 3(b).

V. Experimental Results

Experimental 25-W, 110-V ac-input, single-switch QRLEDD prototype with current doubler rectifier was built and tested.

The circuit parameters and operating conditions were: the LED string voltage $V_{\mathrm{LED}} = 30\,V$; the switching frequency f_s = 150–200 kHz; the on-time $T_{\mathrm{on}} = 1.25\ \mu$s; the input inductance $L_i = 270\ \mu$H; the coupled resonant inductor (with both windings in series): $L_r = 128\ \mu$H; capacitors: $2C_S = 3$ nF; C_b = 22 nF; and $C_{\mathrm{LED}} = 10\ \mu$F.

Experimental results, see Fig. 4(a), confirm that zero-current switching at turn-on of the switch and zero voltage switching at turn-off of the switch were achieved. Line current, shown in Fig. 4(b), is nearly sinusoidal with only 5% distortion, Fig. 4(c).

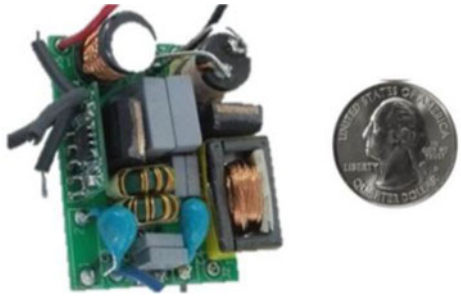

Fig. 6. View of one of the experimental prototypes. LWH = 45×30×30 [mm].

The efficiency plot is shown in Fig. 5, and the size of a 30-W prototype is shown in Fig. 6.

VI. Conclusion

A family of bridgeless and single-switch quasi-resonant LED drivers is introduced. Primary advantages of the proposed topologies are inherently resistive input characteristic, which results in low line-current harmonic content and high power factor. Also zero-voltage switching turn-off, zero-current turn-on are achieved. The proposed topology also realizes capacitive isolation barrier.

One important characteristic of the proposed BL-QRLEDD is the totem-pole configuration. In the past, this type of bridgeless circuit was not popular due to the diode reverse-recovery concerns. BL QRLEDD operates with discontinuous current, which alleviates the reverse-recovery problem. Another modification suggested here was an application of the current doubler rectifiers either discrete or coupled. This allows the current sharing regime of the output rectifier as well as raising the switching frequency and, accordingly, higher output power. The efficiency may be raised by approximately 5%, to exceed 90%, by synchronous rectification (see Fig. 1e). Due to the relatively high-voltage stress the topologies are more suitable for 110-V ac input.

References

[1] J. Y. Tsao, "Solid-state lighting: Lamps, chips, and materials for tomorrow," *IEEE Circuits Devices Mag.*, vol. 20, no. 3, pp. 28–37, May/Jun. 2004.

[2] *Information Technology Equipment—Safety—Part 1: General Requirements*, UL Standard 60950-1, Mar. 27, 2007.

[3] J. Zhu, M. Xu, J. Sun, and C. Wang, "Novel capacitor-isolated power converter," in *Proc. IEEE Energy Convers. Congr. Expo.*, Sep. 12–16, 2010, pp. 1824–1829.

[4] M. Kline, I. Izyumin, B. Boser, and S. Sanders, "A transformerless galvanically isolated switched capacitor LED driver," in *Proc. 27th IEEE Annu. Appl. Power Electron. Conf. Expo.*, Feb. 5–9, 2012, pp. 2357–2360.

[5] A. Abramovitz, I. Reichman, and D. Shmilovitz, "Quasi-resonant LED driver with capacitive isolation," *Electron. Lett.*, vol. 51, no. 3, pp. 274–276, 2015.

[6] D. Shmilovitz, A. Abramovitz, and I. Reichman, "Quasi resonant LED driver with capacitive isolation and high PF," *IEEE J. Emerging Sel. Topics Power Electron.*, vol. 3, no. 3, pp. 633–641, Sep. 2015.

[7] J. Zhang, J. Wang, and X. Wu, "A capacitor-isolated LED driver with inherent current balance capability," *IEEE Trans. Ind. Electron.*, vol. 59, no. 4, pp. 1708–1716, Apr. 2012.

[8] D. Shmilovitz, "Gyrator realization based on a capacitive switched cell," *IEEE Trans. Circuits Syst. II*, vol. 53, no. 12, pp. 1418–1422, Dec. 2006.

[9] D. Shmilovitz, I. Yaron, and S. Singer, "Transmission-line based gyrator," *IEEE Trans. Circuits Syst. I*, vol. 45, no. 4, pp. 428–433, Apr. 1998.